Astrophysical S-factor of ^{14}N(p,γ)^{15}O*

A.Formicola,[1] G.Imbriani,[2] H.Costantini,[3] C.Angulo,[4] D.Bemmerer,[5] R.Bonetti,[6] C.Broggini,[7] P.Corvisiero,[3] J.Cruz,[8] P.Descouvemont,[9] Z.Fülöp,[10] G.Gervino,[11] A.Guglielmetti,[12] C.Gustavino,[13] G.Gyürky,[10] A.P.Jesus,[8] M.Junker,[13] A.Lemut,[3] R.Menegazzo,[7] P.Prati,[3] V.Roca,[14] C.Rolfs,[1] M.Romano,[14] C.Rossi Alvarez,[7] F.Schümann,[1] E.Somorjai,[10] O.Straniero,[15] F.Strieder,[1] F.Terrasi,[16] H.P.Trautvetter,[1] A.Vomiero,[17] and S.Zavatarelli[3]

[1]*Institut für Experimentalphysik III, Ruhr-Universität Bochum, Bochum, Germany*
[2]*Osservatorio Astronomico di Collurania, Teramo and INFN Napoli*
[3]*Università di Genova, Dipartimento di Fisica and INFN, Genova*
[4]*Centre de Recherches du Cyclotron, Universit catholique de Louvain, Louvain-la-Neuve, Begium*
[5]*Institut für Atomare Physik und Fachdidaktik, Technische-Universitt Berlin, Germany*
[6]*Università di Milano, Istituto di Fisica and INFN, Milano, Italy*
[7]*INFN Padova, Italy*
[8]*Centro de Fisica Nuclear da Universidade de Lisboa, Lisboa, Portugal*
[9]*Physique Nuclaire Thorique et Physique Mathmatique, Universite Libre de Bruxelles, Brussels, Belgium*
[10]*Atomki, Debrecen, Hungary*
[11]*Università di Torino, Dipartimento di Fisica Sperimentale and INFN, Torino, Italy*
[12]*Università di Milano, Dipartimento di Fisica and INFN, Milano, Italy*
[13]*INFN Laboratori Nazionali del Gran Sasso, Assergi, Italy*
[14]*Università di Napoli, Dipartimento di Fisica and INFN, Napoli, Italy*
[15]*Osservatorio Astronomico di Collurania, Teramo, Italy*
[16]*Seconda Università di Napoli, Dipartimento di Scienze Ambientali, Caserta, and INFN Napoli, Italy*
[17]*Università di Padova, Dipartimento di Fisica, Padova and INFN Legnaro, Italy*

(Dated: February 5, 2004)

We report on a new measurement of the ^{14}N(p,γ)^{15}O capture cross section at $E_p = 140$ to 400 keV using the 400 kV LUNA accelerator facility. The uncertainties have been reduced with respect to previous measurements and their analysis. We have analyzed the data using the R-matrix method and we find that the ground state transition accounts for about 15% of the total S-factor. The main contribution to the S-factor is given by the transition to the 6.79 MeV state. We find a total $S(0) = 1.7 \pm 0.2$ keV b, in agreement with recent results.

PACS numbers: 24.30.-v, 24.50+g, 26.20.+f

The capture reaction ^{14}N(p,γ)^{15}O ($Q = 7297$ keV) is the slowest process in the hydrogen burning CNO cycle [1] and thus of high astrophysical interest. This reaction plays a role of setting the energy production and neutrino spectrum of the sun [2] as well as the age determination of globular clusters [3]. Below 2 MeV, several ^{15}O states contribute to the ^{14}N(p,γ)^{15}O cross section: a $J^\pi = 3/2^+$ subthreshold state at $E_R = -507$ keV ($E_x = 6.79$ MeV), and 3 resonant states: $J^\pi = 1/2^+$ at $E_R = 259$ keV, and $3/2^+$ at $E_R = 989$ keV and $E_R = 2187$ keV. The reaction was previously studied over a wide range of energies, i.e. $E_{cm} = E = 240$ to 3300 keV ([4] and references therein). The non resonant capture to excited states in ^{15}O led the authors of ref. [4] to an extrapolated astrophysical S-factor at zero energy of $S_{es}(0) = 1.65$ keV b. The data for the capture into the ^{15}O ground state were analyzed using the Breit-Wigner formalism and indicated an important influence of a subthreshold state at $E_R = -507$ keV, leading to $S_{gs}(0) = 1.55$ keV b with a deduced gamma width of $\Gamma_\gamma = 6.3$ eV, thus $S_{tot}(0) = 3.2$ keV b.

A reanalysis of the capture data to the ground state [4] using an R-matrix approach indicated [5] a negligible contribution of the subthreshold state to the total S(0)-factor, mainly due to a significantly smaller Γ_γ of this state. This indication was supported by a lifetime measurement of the $E_R = -507$ keV subthreshold state via the Doppler-shift method [6] leading to $\Gamma_\gamma = 0.41^{+0.34}_{-0.13}$ eV and a measurement via the Coulomb excitation method [7] resulted in $\Gamma_\gamma = 0.95^{+0.6}_{-0.95}$ eV. In view of the uncertainties in $S_{gs}(0)$ and thus $S_{tot}(0)$, a new measurement of the capture process into the ^{15}O ground state was highly desirable, extending possibly the low energy limit below that of previous work i.e., below $E = 240$ keV. We report on the results of such measurements using the 400 kV underground accelerator facility LUNA at Gran Sasso, Italy.

The 400 kV LUNA facility and the setup have been described elsewhere [8]. Briefly, the accelerator provided a proton current on target of up to 500 μA. The absolute energy is known with an accuracy of 0.3 keV and the energy spread and the long-term energy stability were observed to be 100 eV and 5 eV/h, respectively. Near the target, the beam passed a liquid-nitrogen cooled shroud

*Supported in part by INFN, BMBF(05CL1PC1), GSI(BO-ROL), OTKA(T034259 and T042733), TARI HPRI-CT-2001-00149 and SSTC PAI(P5/07)

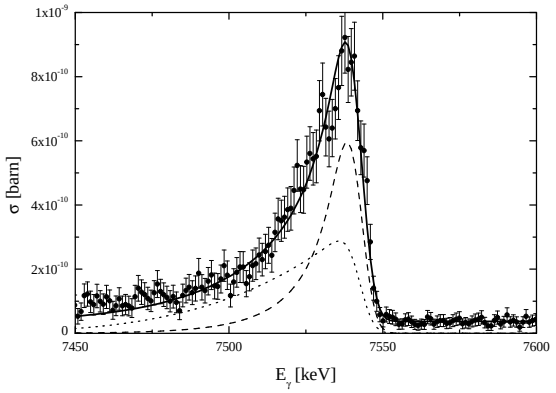

FIG. 1: Typical γ_0-ray line shape of ^{14}N(p,γ)^{15}O obtained at $E_p = 260$ keV. The dashed line corresponds to the expected resonant part, the dotted line to the fitted non-resonant part, and the solid line is their sum including background.

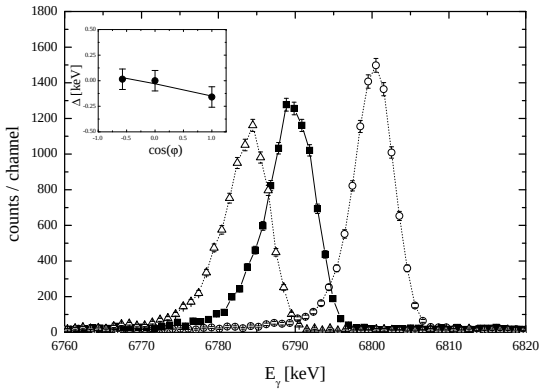

FIG. 2: Full-energy peak for the 6791 → 0 transition observed with three Ge detectors positioned at 0° (open circles), 90° (filled squares), and 125° (open triangles). The insert shows the measured energy shift relative to the expected full Doppler shift, where the solid line corresponds to the attenuation factor $F(\tau) = 0.99$.

(to minimize carbon-buildup on target) and an electrically insulated collimator with a negative voltage of 300 V (to suppress the effects of secondary electrons). The water-cooled target was oriented with its normal at 55° to the beam direction. The target consisted of a TiN layer (with a typical thickness of 80 keV) reactively sputtered on a 0.2 mm thick Ta backing. The target quality was checked frequently at the $E_R = 259$ keV resonance: no significant deterioration was observed after a bombarding time of several days. Typically, a new TiN target was used after a running time of 1 week. The stoichiometry of the TiN layer was verified via Rutherford Backscattering Spectrometry using a 2.0 MeV ^{4}He$^+$ beam, resulting in $Ti/N = 1/(1.08 \pm 0.05)$.

For the measurement of excitation functions the capture γ-rays were observed with one Ge detector (126% efficiency) placed at 55° in close geometry to the target ($d = 1.53$ cm was the distance between the target and the front face of the detector). In one experiment the distance was increased up to 20.5 cm for the determination of the detector efficiency and summing effects. In another experiment, Ge detectors were placed at 0° (126 %), 90° (120 %), and 125° (108 %), relative to the beam axis ($d = 7$ cm) for the measurement of Doppler shifts, excitation energies, and angular distributions.

In a similar way as described in [8], the line shape of the γ_0-capture transition in ^{14}N(p,γ)^{15}O may be used for various purposes. Fig. 1 shows the γ_0-ray line shape observed at $\theta_\gamma = 55°$ and $E = 243$ keV, i.e. at the low-energy tail of the $E_R = 259$ keV resonance; the dispersion in the spectrum was 1 keV/channel. The line shape can be interpreted as the sum of the resonant and non resonant contributions; when convoluted with the detector resolution, the solid curve through the data points is obtained. In this way, the drop in the γ_0-ray yield towards lower energies reflects directly the drop of the cross section. For the calculated line shape the dependence on energy of the γ_0-efficiency and of the stopping power of protons in TiN [10] was included. The high-energy edge of the peak contains the information on the incident beam energy, hence possible C-build up on target could be corrected for; this correction was never larger than 2 keV. The method to extract the cross section from the γ_0-ray line shape requires further investigation of the following points: (i) energy, width, branching ratios, and strength of the $E_R = 259$ keV resonance, (ii) energy calibration and efficiency of the Ge detector, (iii) summing effects in close geometry, (iv) Doppler shift, and (v) effects of angular distributions. In the same way the transition to the 6.79 MeV state was analysed. Below $E = 170$ keV the information of the data from the secondary transition was used in the analysis. For this energy region a constant $S_{6.79}$ was assumed over the target thickness. A detailed description of all these points is given elsewhere [11, 12], where a complete analysis of the data to all final states will be presented.

The resonance energy could in principle be determined from the γ_0-energy after correction for Doppler shift and recoil. One requirement is the precise energy calibration of the Ge detector. We have used the information obtained from the experiment with the 3 Ge detectors ($\theta_\gamma = 0°$, 90°, and 125°). From [6] it is known, that the $E_x = 5181$ keV state in ^{15}O shows an attenuated Doppler shift and the 6172 and 6790 keV states have lifetimes resulting in nearly full Doppler shifts. Using the known energy of the resonance from the accelerator calibration together with $Q = 7296.8 \pm 0.5$ keV [13] and calibration points from radioactive sources we have performed a combined χ^2 fit of the data obtained at the three angles. It was necessary to vary also the excitation energies of the first three excited states. In addition, we varied the attenuation coefficients for the Doppler shifts.

TABLE I: Excitation energies in ^{15}O, Doppler shift measurements and γ-branching ratios for the 259 keV resonance (E_x = 7556 keV).

E_x [keV]		$F(\tau)$ Doppler shift		Branching [%][a]	
present	[9]	present[b]	[6][c]	present	[9]
5180.51 ± 0.14	5183.0 ± 1.0	0.68 ± 0.03	0.68 ± 0.03	16.6 ± 0.2	15.8 ± 0.5
6171.86 ± 0.15	6176.3 ± 1.7	0.99 ± 0.03	0.91 ± 0.05	58.4 ± 0.3	57.5 ± 0.6
6791.23 ± 0.19	6793.1 ± 1.7	0.99 ± 0.04	0.93 ± 0.03	23.3 ± 0.3	23.2 ± 0.4
7556.23 ± 0.28	7556.5 ± 0.4			1.67 ± 0.1[d]	3.5 ± 0.6[d]

[a] for the $E_R = 259$ keV resonance
[b] TiN target
[c] N implanted in Ta
[d] transition to the ground state

The Doppler shift data for the $E_x = 6791$ keV state are shown in Fig. 2 and all results are summarized in Table I. We confirm the results of [6] for the first excited state in ^{15}O but could not extract a lifetime for the 6791 keV state due to a nearly full Doppler shift. For all the subsequent work we calibrated the γ-ray spectra using the new excitation energies given in Table I.

The detector efficiency was determined using calibrated radioactive sources and the cascade condition for the transitions to the first three excited states at the $E_R = 259$ keV resonance, as for all of them no other decay than that to the ground state was observed. This procedure was performed with the Ge detector placed at 1.53, 5.5, 10.5, and 20.5 cm distances from the target in order to determine the summing-in contribution to the ground state transition and the summing-out for the transitions to the excited states. It turned out, that the summing-in yield was about 3.5 times higher than the actual ground state intensity at the 1.53 cm position. This 1.53 cm position was used for the entire cross section measurements. The efficiency curve was also calculated using the GEANT routine [14] and found to be in excellent agreement with observation [11]. Branching and strength values of the $E_R = 259$ keV resonance were determined with low beam current to avoid dead time effects and at far distance (20.5 cm) to minimize summing effects from cascade transitions. The branching results are given in Table I; they are in good agreement with previous work [15], except for the ground state transition. Our strength value of $\omega\gamma = 13.5 \pm 0.4$ (statistical) ± 0.8(systematical) meV is also in good agreement with previous work [4, 9], $\omega\gamma = 14 \pm 1$ meV. All transitions show isotropy at the $E_R = 259$ keV, $J = 1/2$ resonance and no forward-backward asymmetry [11] outside the resonance. Consequently, an angle-integrated γ_0-ray yield may be derived directly from the yield collected by the Ge detector at $\theta_\gamma = 55°$. Finally, the summing due to the large solid angle of the detector and the cascade coincident events in the transition to the ground state was corrected for by studying all other capture transitions.

First fits of the LUNA data with an R-matrix approach [5, 16] including only the subthreshold state, the 259 keV resonance and a background pole resulted in an extrapolated value $S_{gs}(0) = 0.27$ keV b for the ground state transition. Including the data of [4] the extrapolated value was reduced by a factor of 3 indicating the importance of the energy regime above the 259 keV resonance. The data of [4] were partly based on the branching ratio for the ground state transition of the 259 keV resonance as reported in [15], where it was noted that considerable summing could be expected for the detector-setup used. We have corrected these data for summing with the result of a change in the $E_R = 259$ keV branching ratio for the ground state transition to be 1.8 % in excellent agreement with the present result of 1.65 %. The correction factor for the data of [4] is at most 10 % above $E = 500$ keV except near the destructive interference structure of the $E_R = 987$ keV resonance. One other aspect was to exclude the S-factor values of [4] near the $E_R = 259$ keV resonance since they represent integrated values over the target thickness. The value at the 259 keV resonance for the LUNA data was obtained from the measured $\omega\gamma$ value and the fitted total width $\Gamma = 0.99 \pm 0.03$ keV of the resonance ([4]: $\Gamma = 1.2 \pm 0.2$ keV).

Details for the procedure of the R-matrix fit can be found in [5]. The fit was done in two steps. First the transition to the 6.79 MeV state was fitted including the data set given by [4], which is in excellent agreement with the present results (Fig. 3) in the region of overlap. As known from previous work [4, 5] the S-factor has an external non-resonant contribution and a resonant contribution from the $E_x = 7.56$ MeV state ($E_R = 259$ keV). As expected, the resulting ANC value deduced from the capture data is not very sensitive to the R-matrix radius a and results in $C = 5.0 \pm 0.1$ fm$^{-1/2}$ in good agreement with [17] ($C = 5.2 \pm 2.6$ fm$^{-1/2}$) and [18] ($C = 4.6 \pm 2.2$ fm$^{-1/2}$). The R-matrix fit for the transition to the 6.79 MeV state is shown in Fig. 3. For large values of the radius a the fit deviates from the data for energies above $E = 1$ MeV (Fig. 3). We have adopted the results for $a = 5.5$ fm and the extrapolation of the corresponding S(E) value results in $S_{6.79}(0) = 1.35 \pm 0.05$ (statistical) ± 0.08 (systematical) ke-b . This value is about 20 % lower than the R-matrix fit [5] of the data from [4] alone.

As the next step, we analysed the LUNA data together

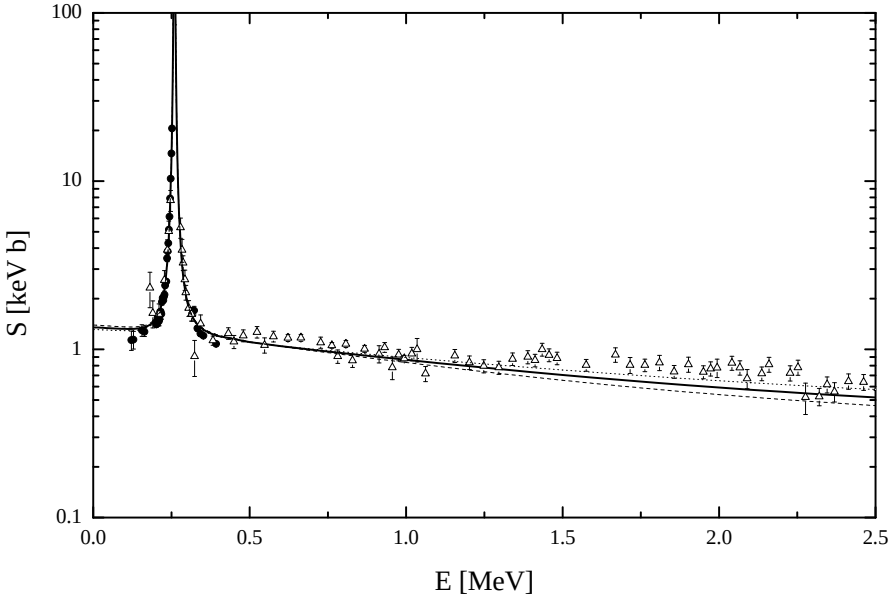

FIG. 3: Transition to the 6.79 MeV state in ^{15}O. The S-factor data from previous work are represented by solid points, those of [4] by open triangles. The R-matrix fit (solid line) was obtained for $a = 5.5$ fm, the dashed line for $a = 6$ fm and the dotted line for $a = 5$ fm. The data point in the 259 keV resonance is off scale.

TABLE II: R-matrix parameters for capture transition to the ground state

	ground state	subthreshold state		E_{res}		transition to	
radius	ANC			2.19 MeV	6 MeV	$E_x = 0$ MeV	$E_x = 6.79$ MeV
a [fm]	C [fm$^{-1/2}$]	γ^2 [MeV]	Γ_γ [eV]	Γ_γ [eV]	Γ_γ [eV]	S(0) [keV b]	S(0) [keV b]
5	5.8	0.40	1.2	4.3	25	0.19	1.31
5.5	7.34	0.42	0.78	4.4	23	0.25	1.35
6	8.8	0.44	0.51	4.7	26	0.31	1.39
average		0.42 ± 0.02	0.8 ± 0.4	4.5 ± 0.2	23 ± 3	0.25 ± 0.06	1.35 ± 0.05

with the data from [4] for the ground state transition, including the $3/2^+$ subthreshold state, the $1/2^+$, 259 keV, the $3/2^+$, 989 keV and the $3/2^+$, 2187 MeV resonances as well as a background pole located at 6 MeV. For the subthreshold state, we used the reduced width γ^2 obtained from the fit of the data for the 6.79 MeV transition. The fit parameters were the Γ_γ of the subthreshold state, the 989 keV and 2187 MeV resonances, the Γ_p and Γ_γ of the background pole. For the external contribution we used the ANC of [17] as a starting value.

The results are shown in Fig. 4 for $a = 5$ fm and $C_{gs} = 5.8$ fm$^{-1/2}$ (dotted line), $a = 5.5$ fm and $C_{gs} = 7.3$ fm$^{-1/2}$ (solide line), and $a = 6.5$ fm and $C_{gs} = 8.8$ fm$^{-1/2}$ (dashed line). The corresponding Γ_γ values for the subthreshold state and extrapolated S-factor values are listed in Table II. It can be noted that our deduced value $\Gamma_\gamma = 0.8 \pm 0.4$ eV is in good agreement with the value from a life time measurement by [6] $\Gamma_\gamma = 0.41^{+0.34}_{-0.13}$ eV as well as with $\Gamma_\gamma = 0.95^{+0.6}_{-0.95}$ eV, the value from coulomb excitation work [7]. All Γ_γ values from Table II are consistent within uncertainties with our observation of a nearly full Doppler shift of the transition to the 6.79 MeV state (see Fig. 2). The best χ^2 for the fit to the ground state transition is obtained for $a = 6$ fm ($\chi^2 = 1.27$), however the differences are small (for $a = 5$, $\chi^2 = 1.35$ (Contributions to χ^2 near the narrow resonances have been omitted in the χ^2 values given above). The best overall agreement with all available data [4, 6, 7, 17, 18] is obtained for $a = 5.5$ fm, where our fitted ground state ANC is $C = 7.3$ fm$^{-1/2}$, that can be compared with the result of [17] which gives $C = 7.3 \pm 0.4$ fm$^{-1/2}$, after conversion to the coupling scheme used in the present work. For the total S-factor a contribution from the transition to the 6.18 MeV state of $S_{6.18}(0) = 0.06$ keV b from [5] has been added to obtain an average ($a = 5$ to 6 fm) of $S_{tot}(0) = 1.7 \pm 0.1$ (statistical) ± 0.2(systematical) keV b, which can be compared

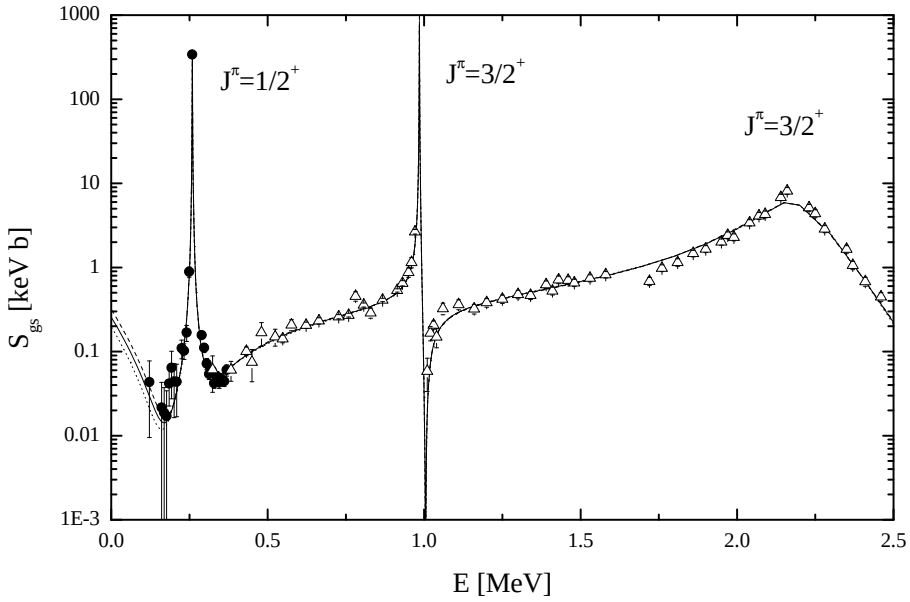

FIG. 4: Astrophysical S(E)-factor curve for the ground state transition in ^{14}N(p,γ)^{15}O. Filled-in data points are the results from LUNA, while the open data points are from previous work [4] correct for summing effects. The solid line corresponds to the R-matrix fit for $a = 5.5$ fm, the dashed line for $a = 6$ fm and the dotted line for $a = 5$ fm.

with 1.77 ± 0.2 keV b [5] and 1.70 ± 0.22 keV b [17] from previous analyses.

In summary, the present work improves the experimental information concerning the ground state transition in ^{14}N(p,γ)^{15}O. The previous data [4] corrected by summing effects discussed above are now in good agreement with the present work. The large ambiguity for the extrapolation of the ground state transition has been reduced. In the energy region between $E = 170$ to 300 keV the S(E)-factor is dominated by the 259 keV resonance. Only at energies of about 100 keV and below the contributions of the subthreshold resonance and non-resonant mechanisms should become clearly observable. Using large volume Ge detectors it is impossible to obtain additional information on S_{gs}(E) at lower energies (than current work) with acceptable uncertainty due to the sizable summing correction. An improved information on S_{tot}(E) can be achieved possibly using a 4π-summing crystal to observe the total S(E)-factor. Such an experiment is presently underway at the LUNA facility.

[1] C.Rolfs and W.S.Rodney, *Cauldrons in the Cosmos* (University of Chicago Press, 1988).
[2] J.N.Bahcall and M.H.Pinsonneault, Rev.Mod.Phys. **64**, 885 (1992).
[3] P.A.Bergbusch and B.A.Vandenberg, Ap.J.Suppl **81**, 163 (1992).
[4] U.Schröder et al., Nucl.Phys. A **467**, 240 (1987).
[5] C.Angulo and P.Descouvement, Nucl.Phys.A. **690**, 755 (2001).
[6] P.F.Bertone et al., Phys.Rev.Lett. **87**, 152501 (2001).
[7] K.Yamada et al. (2003), RIKEN-AF-NP-451 and accepted by Phys. Lett. B.
[8] A.Formicola et al., Nucl.Instr.Meth. A **507**, 609 (2003).
[9] F.Ajzenberg-Selove, Nucl. Phys. A **523**, 1 (1991).
[10] J.F.Ziegler and J. Biersack, *Srim-program, version 2003-20, srim.org* (2003).
[11] H.Costantini (2003), Thesis, University of Genova and to be published.
[12] A.Formicola, *Thesis* (Ruhr-Universität Bochum, 2004).
[13] G.Audi, A.H.Wapstra, and C.Thibault, Nucl. Phys. A **729**, 337 (2003).
[14] GEANT4: An Object-Oriented Toolkit for Simulation in HEP. The RD44 Collaboration, CERN/LHCC 95-70, 1995 and The Geant4 Collaboration, http://wwwinfo.cern.ch/asd/geant4/geant4.html.
[15] D.F.Hebbard and G.M.Bailey, Nuc. Phys. **49**, 666 (1963).
[16] A.N.Lane and R.G.Thomas, Rev. Mod. Phys. **36**, 257 (1958).
[17] A.M.Mukhamedzhanov et al., Phys. Rev. C **67**, 065804 (2003).
[18] P.F.Bertone et al., Phys.Rev. C **66**, 055804 (2002).